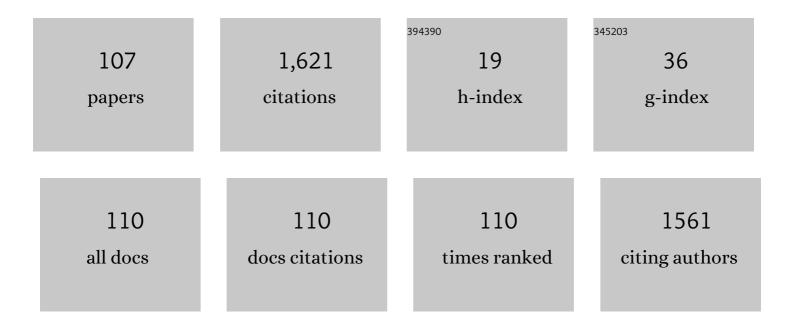
Javier Miranda

List of Publications by Year in descending order

Source: https://exaly.com/author-pdf/9453057/publications.pdf Version: 2024-02-01



#	Article	IF	CITATIONS
1	Proinflammatory and cytotoxic effects of Mexico City air pollution particulate matter in vitro are dependent on particle size and composition Environmental Health Perspectives, 2003, 111, 1289-1293.	6.0	243
2	Motor alterations associated with exposure to manganese in the environment in Mexico. Science of the Total Environment, 2006, 368, 542-556.	8.0	106
3	Induction of IL-6 and inhibition of IL-8 secretion in the human airway cell line Calu-3 by urban particulate matter collected with a modified method of PM sampling. Environmental Research, 2009, 109, 528-535.	7.5	78
4	A receptor model for atmospheric aerosols from a southwestern site in Mexico City. Atmospheric Environment, 1996, 30, 3471-3479.	4.1	71
5	In vitro biological effects of airborne PM2.5 and PM10 from a semi-desert city on the Mexico–US border. Chemosphere, 2011, 83, 618-626.	8.2	68
6	Organic compounds of PM2.5 in Mexico Valley: Spatial and temporal patterns, behavior and sources. Science of the Total Environment, 2011, 409, 1453-1465.	8.0	62
7	Determination of elemental concentrations in atmospheric aerosols in mexico city using proton induced x-ray emission, proton elastic scattering, and laser absorption. Atmospheric Environment, 1994, 28, 2299-2306.	4.1	60
8	Experimental cross sections for L-shell x-ray production and ionization by protons. Atomic Data and Nuclear Data Tables, 2014, 100, 651-780.	2.4	58
9	Airborne particulate matter in vitro exposure induces cytoskeleton remodeling through activation of the ROCK-MYPT1-MLC pathway in A549 epithelial lung cells. Toxicology Letters, 2017, 272, 29-37.	0.8	31
10	DEVELOPMENT OF AN X-RAY FLUORESCENCE SPECTROMETER FOR ENVIRONMENTAL SCIENCE APPLICATIONS. Instrumentation Science and Technology, 2012, 40, 603-617.	1.8	30
11	Cytoplasmic p21CIP1/WAF1, ERK1/2 activation, and cytoskeletal remodeling are associated with the senescence-like phenotype after airborne particulate matter (PM10) exposure in lung cells. Toxicology Letters, 2014, 225, 12-19.	0.8	29
12	TWO YEAR STUDY OF ELEMENTAL COMPOSITION OF ATMOSPHERIC AEROSOLS IN MEXICO CITY. International Journal of PIXE, 1991, 01, 373-388.	0.4	27
13	Absolute principal component analysis of atmospheric aerosols in Mexico city. Environmental Science and Pollution Research, 2000, 7, 14-18.	5.3	25
14	Ice-nucleating particles in a coastal tropical site. Atmospheric Chemistry and Physics, 2019, 19, 6147-6165.	4.9	25
15	Measurement of L X-ray production cross sections by 400–700 keV proton impact on rare earth elements. Nuclear Instruments & Methods in Physics Research B, 1993, 75, 49-53.	1.4	24
16	Low energy PIXE: advantages, drawbacks, and applications. Nuclear Instruments & Methods in Physics Research B, 1996, 118, 346-351.	1.4	24
17	PIXE analysis of atmospheric aerosols from three sites in Mexico City. Nuclear Instruments & Methods in Physics Research B, 2004, 219-220, 157-160.	1.4	24
18	Uses of PIXE at low proton energies. Applied Surface Science, 1990, 45, 155-166.	6.1	23

#	Article	IF	CITATIONS
19	Measurement of M-shell X-ray production induced by protons of 0.3–0.7 MeV on W, Au, Pb, Bi, Th and U. Nuclear Instruments & Methods in Physics Research B, 2002, 189, 27-32.	1.4	21
20	Effect of atomic parameters on L-shell X-ray production cross-sections by proton impact with energies below 1 MeV. Nuclear Instruments & Methods in Physics Research B, 2002, 189, 21-26.	1.4	20
21	Multiple ionization effects on total L-shell X-ray production cross sections by proton impact. Radiation Physics and Chemistry, 2004, 69, 257-263.	2.8	18
22	Recognition of the importance of geogenic sources in the content of metals in PM2.5 collected in the Mexico City Metropolitan Area. Environmental Monitoring and Assessment, 2018, 190, 83.	2.7	18
23	PIXE analysis of atmospheric aerosols in Mexico City. X-Ray Spectrometry, 2005, 34, 315-319.	1.4	17
24	The oxidative potential and biological effects induced by PM10 obtained in Mexico City and at a receptor site during the MILAGRO Campaign. Environmental Pollution, 2011, 159, 3446-3454.	7.5	17
25	SURVEY OF PIXE PROGRAMS — 1991. International Journal of PIXE, 1991, 01, 297-310.	0.4	16
26	Characterization of pre-Hispanic pottery from Teotihuacan, Mexico, by a combined PIXE–RBS and XRD analysis. Nuclear Instruments & Methods in Physics Research B, 1999, 150, 591-596.	1.4	16
27	K X-ray emission induced by 12C4+ and 16O5+ ion impact on selected lanthanoids. Nuclear Instruments & Methods in Physics Research B, 2009, 267, 1767-1771.	1.4	16
28	Measurement of L X-ray production cross sections by impact of proton beams on Hf, Ir, and Tl. Nuclear Instruments & Methods in Physics Research B, 2013, 316, 113-122.	1.4	16
29	Total elemental composition of soils contaminated with wastewater irrigation by combining IBA techniques. Nuclear Instruments & Methods in Physics Research B, 2002, 189, 158-162.	1.4	15
30	African dust particles over the western Caribbean – Part I: Impact on air quality over the Yucatán Peninsula. Atmospheric Chemistry and Physics, 2021, 21, 239-253.	4.9	15
31	Atmospheric PM2.5 Mercury in the Metropolitan Area of Mexico City. Bulletin of Environmental Contamination and Toxicology, 2018, 100, 588-592.	2.7	14
32	A study of atmospheric aerosols from five sites in Mexico city using PIXE. Nuclear Instruments & Methods in Physics Research B, 1998, 136-138, 970-974.	1.4	13
33	L-shell X-ray production cross section measured by heavy ion impact on selected rare earth elements. Journal of Radioanalytical and Nuclear Chemistry, 2004, 262, 391-401.	1.5	13
34	lon beam analysis of pottery from Teotihuacan, Mexico. Nuclear Instruments & Methods in Physics Research B, 2000, 161-163, 762-768.	1.4	12
35	X-Ray Fluorescence Analysis of Ground Coffee Journal of Nuclear Physics Material Sciences Radiation and Applications, 2017, 5, 25-34.	0.2	12
36	A comparison between pixe and rbs thin film thickness measurements in binary targets. Nuclear Instruments & Methods in Physics Research B, 1987, 29, 521-526.	1.4	11

#	Article	IF	CITATIONS
37	Studies of atmospheric aerosols in large urban areas using PIXE: an overview. Nuclear Instruments & Methods in Physics Research B, 1996, 109-110, 439-444.	1.4	11
38	Characterization of aerosol particles during a high pollution episode over Mexico City. Scientific Reports, 2021, 11, 22533.	3.3	11
39	PIXE depth profiling using variation of detection angle. Nuclear Instruments & Methods in Physics Research B, 2006, 249, 394-396.	1.4	10
40	Simultaneous PIXE and XRF elemental analysis of atmospheric aerosols. Microchemical Journal, 2015, 120, 40-44.	4.5	10
41	Spatial and temporal distribution of metals in PM2.5 during 2013: assessment of wind patterns to the impacts of geogenic and anthropogenic sources. Environmental Monitoring and Assessment, 2019, 191, 165.	2.7	10
42	L-Shell X-ray production cross-sections by impact of 5.0 to 7.5 MeV 10B2+ ions on selected rare earth elements. Nuclear Instruments & Methods in Physics Research B, 2004, 219-220, 289-293.	1.4	9
43	K X-ray production by 12C4+ ion impact on selected elements. Radiation Physics and Chemistry, 2005, 73, 189-195.	2.8	9
44	L-shell alignment of rare earths atoms induced by 12C, 16O and 19F ion impact. Nuclear Instruments & Methods in Physics Research B, 2006, 248, 47-53.	1.4	9
45	Measurement of K–L radiative vacancy transfer probabilities in selected rare earth elements bombarded with 3–4MeV protons. Nuclear Instruments & Methods in Physics Research B, 2008, 266, 5075-5079.	1.4	9
46	PIXE and XRF analysis of atmospheric aerosols from a site in the West area of Mexico City. Nuclear Instruments & Methods in Physics Research B, 2014, 318, 135-138.	1.4	9
47	Ion beam analysis of ancient Mexican colored teeth from archaeological sites in Mexico City. Nuclear Instruments & Methods in Physics Research B, 1999, 150, 663-666.	1.4	8
48	The possible influence of volcanic emissions on atmospheric aerosols in the city of Colima, Mexico. Environmental Pollution, 2004, 127, 271-279.	7.5	8
49	The use of biomonitors and PIXE analysis in the study of air pollution in Mexico City. X-Ray Spectrometry, 2008, 37, 156-162.	1.4	8
50	Universal empirical fit to L-shell X-ray production cross sections in ionization by protons. Nuclear Instruments & Methods in Physics Research B, 2018, 414, 184-189.	1.4	8
51	The role of the ionization and stopping cross sections in PIXE thin film thickness measurements. Nuclear Instruments & Methods in Physics Research B, 1988, 34, 362-368.	1.4	7
52	L-shell X-ray production cross sections of selected lanthanoids by impact of 7Li2+ ions with energies between 3.50MeV and 5.25MeV. Radiation Physics and Chemistry, 2013, 83, 48-53.	2.8	7
53	L-shell X-ray production cross sections of Ce, Nd, Sm, Eu, Gd, and Dy by impact of 14 N 2+ ions with energies between 7.0 MeV and 10.5 MeV. Nuclear Instruments & Methods in Physics Research B, 2016, 383, 89-92.	1.4	7
54	Measurement report: Ice nucleating abilities of biomass burning, African dust, and sea spray aerosol particles over the Yucatán Peninsula. Atmospheric Chemistry and Physics, 2021, 21, 4453-4470.	4.9	7

#	Article	IF	CITATIONS
55	ADABBOY: African Dust And Biomass Burning Over Yucatan. Bulletin of the American Meteorological Society, 2021, 102, E1543-E1556.	3.3	7
56	The use of a Perovskite crystal as a detector for proton beam current. IEEE Transactions on Nuclear Science, 1992, 39, 25-28.	2.0	6
57	PIXE analysis of cave sediments, prehispanic paintings and obsidian cutting tools from Baja California Sur caves. Nuclear Instruments & Methods in Physics Research B, 1993, 75, 454-457.	1.4	6
58	L-subshell X-ray production by 400–700 keV protons in selected elements with 52 â‰⊄ â‰⊄1. Nuclear Instruments & Methods in Physics Research B, 1994, 85, 150-153.	1.4	6
59	Analysis of diatomite sediments from a paleolake in central Mexico using PIXE, X-ray tomography and X-ray diffraction. Nuclear Instruments & Methods in Physics Research B, 1994, 85, 886-889.	1.4	6
60	Characterization of a Si(Li) detector for PIXE analysis. Journal of X-Ray Science and Technology, 1994, 4, 221-246.	1.0	6
61	Application of PIXE and XRD to the Characterization of Clays. Microchemical Journal, 1995, 52, 356-363.	4.5	6
62	Study of prehispanic wall paintings from Xochicalco, Mexico, using PIXE, XRD, SEM and FTIR. Journal of Radioanalytical and Nuclear Chemistry, 1999, 240, 561-569.	1.5	6
63	Total L-shell X-ray production cross sections by 400–700 keV proton impact for elements with 34 ≤ ≤ 53. Applied Radiation and Isotopes, 2001, 54, 455-459.	1.5	6
64	Updated database for <i>L</i> xâ€ray production by protons and extraction of <i>L</i> â€subshell ionization cross sections from only <i>L</i> _γ and <i>L</i> _α + <i>L</i> _β cross sections. X-Ray Spectrometry, 2011, 40, 122-126.	1.4	6
65	Total L X-ray production cross sections of Sr, Y, Zr, Nb, and Mo induced by impact of 1.335†MeV to 1.835†MeV to 1.835†MeV protons. Nuclear Instruments & Methods in Physics Research B, 2020, 477, 23-26.	1.4	6
66	Improvements to the X-ray Spectrometer at the Aerosol Laboratory, Instituto de FÃsica, UNAM. Journal of Nuclear Physics Material Sciences Radiation and Applications, 2018, 6, 57-60.	0.2	6
67	RESOLUTION IN PIXE THIN FILM THICKNESS DETERMINATION. International Journal of PIXE, 1991, 01, 259-270.	0.4	5
68	Pollution effects on stone benches of the Eagle Warriors Precinct at the Major Temple, Mexico City. Nuclear Instruments & Methods in Physics Research B, 1999, 150, 611-615.	1.4	5
69	Title is missing!. Journal of Radioanalytical and Nuclear Chemistry, 2002, 251, 15-19.	1.5	5
70	Trace element determination in tomato puree using particle induced X-ray emission and Rutherford backscattering. Journal of Radioanalytical and Nuclear Chemistry, 2004, 262, 355-362.	1.5	5
71	K X-ray production by 3–4MeV proton impact on selected lanthanoids. Radiation Physics and Chemistry, 2010, 79, 1013-1017.	2.8	5
72	Present status of L-shell X-ray production cross sections by protons with energies below 1 MeV. AIP Conference Proceedings, 2001, , .	0.4	4

#	Article	IF	CITATIONS
73	Chemical effects in the stopping cross sections of protons in rare earth fluorides. Nuclear Instruments & Methods in Physics Research B, 2007, 254, 39-42.	1.4	4
74	X-ray fluorescence analysis of Mexican varieties of dried chili peppers II: Commercial and home-grown specimens. AIP Conference Proceedings, 2015, , .	0.4	4
75	Temporal variation of suspended particles (TSP, PM10, and PM2.5) and chemical composition of PM10 in a site at the coast of the Gulf of Mexico. Air Quality, Atmosphere and Health, 2019, 12, 1267-1277.	3.3	4
76	Elemental analysis of PM10 in southwest Mexico City and source apportionment using positive matrix factorization. Journal of Atmospheric Chemistry, 2022, 79, 167-198.	3.2	4
77	A new method for thin-film thickness measurement using PIXE. Nuclear Instruments & Methods in Physics Research B, 1989, 43, 203-209.	1.4	3
78	NdF3 thin films grown on carbon substrates and analyzed by RBS, PIXE, RNRA, SEM and X-ray diffraction. Nuclear Instruments & Methods in Physics Research B, 1993, 79, 471-473.	1.4	3
79	PIXE and RBS elemental analyses of tree rings from Mexico Basin forests as a record of pollution. AIP Conference Proceedings, 2003, , .	0.4	3
80	Evaluation of L-shell X-ray production cross sections by impact of [sup 4]He[sup +] ions. , 2013, , .		3
81	Measurement of L X-ray production cross sections of Ce, Nd, Sm, Eu, Gd, and Dy by impact of 9Be2+ ions with energies in the interval 5.25 MeV to 6.75 MeV. Nuclear Instruments & Methods in Physics Research B, 2018, 434, 93-96.	1.4	3
82	PIXE and XRF elemental analysis of breakfast cereals consumed in Mexico. Journal of Radioanalytical and Nuclear Chemistry, 2018, 318, 887-895.	1.5	3
83	Platinum concentration in PM2.5 in the Mexico City Metropolitan Area: relationship to meteorological conditions. Human and Ecological Risk Assessment (HERA), 2020, 26, 1164-1174.	3.4	3
84	Elemental characterization and risk assessment of indoor aerosols in an electrostatic particle accelerator laboratory. Environmental Pollutants and Bioavailability, 2021, 33, 334-346.	3.0	3
85	Quantification of indium in steel using PIXE. Nuclear Instruments & Methods in Physics Research B, 1989, 40-41, 627-629.	1.4	2
86	Influence of energy straggling on quantitative PIXE analysis. Nuclear Instruments & Methods in Physics Research B, 1996, 109-110, 121-124.	1.4	2
87	L-Shell X Ray Production Cross-sections by 12C4+ and 16O4+ Impact on Rare Earth Elements. AIP Conference Proceedings, 2003, , .	0.4	2
88	lonoluminscence of partially-stabilized zirconia for thermal barrier coatings. Nuclear Instruments & Methods in Physics Research B, 2007, 261, 461-465.	1.4	2
89	Urban particulate matter induces the expression of receptors for early and late adhesion molecules on human monocytes. Environmental Research, 2018, 167, 283-291.	7.5	2
90	Characterization of a Si(Li) Detector for PIXE Analysis. Journal of X-Ray Science and Technology, 1994, 4, 221-246.	1.0	1

#	Article	IF	CITATIONS
91	Effects of perturbations on diatom assemblages in Tlaxcala Paleolake, Mexico. Verhandlungen Der Internationalen Vereinigung Fur Theoretische Und Angewandte Limnologie International Association of Theoretical and Applied Limnology, 1997, 26, 846-851.	0.1	1
92	Origin of laminations in Tlaxcala Paleolake, Mexico. Verhandlungen Der Internationalen Vereinigung Fur Theoretische Und Angewandte Limnologie International Association of Theoretical and Applied Limnology, 1997, 26, 838-841.	0.1	1
93	John L. Campbell. X-Ray Spectrometry, 2008, 37, 94-94.	1.4	1
94	Measurement of Lα and Lβ1,3,4 fluorescence cross sections of La, Ce, Pr and Nd induced by photons of energies between 7.01keV and 8.75keV. Radiation Physics and Chemistry, 2016, 123, 122-128.	2.8	1
95	AMS 14C and Chemical Composition of Atmospheric Aerosols from Mexico City. Radiocarbon, 2017, 59, 321-332.	1.8	1
96	L-shell x-ray production cross sections induced by heavy ion impact: Searching for a universal curve. AIP Conference Proceedings, 2019, , .	0.4	1
97	X-Ray fluorescence analysis of Mexican varieties of dried chili peppers. Journal of Food Composition and Analysis, 2020, 93, 103592.	3.9	1
98	Perspectives for low energy reactions measurements at the new LEMA beam-line. Journal of Physics: Conference Series, 2020, 1643, 012029.	0.4	1
99	X-Ray Fluorescence Analysis of Fine Atmospheric Aerosols from a Site in Mexico City. Journal of Nuclear Physics Material Sciences Radiation and Applications, 2016, 4, 25-30.	0.2	1
100	Analysis of Atmospheric Aerosols in Large Urban Areas with Particle Induced X-ray Emission. , 2000, , 405-413.		1
101	How do Uncertainties in Atomic Parameters Influence Theoretical Predictions of X-Ray Production Cross Sections By Proton Impact?. Journal of Nuclear Physics Material Sciences Radiation and Applications, 2020, 7, 71-76.	0.2	1
102	Studies of atmospheric aerosols in Mexico City using PIXE. , 1997, , .		0
103	Measurement of K-L Radiative Vacancy Transfer Probabilities in Rare Earth Elements Bombarded with [sup 12]C and [sup 16]O lons. , 2009, , .		0
104	New data base for Lα, Lβ, Lγ x-ray production by protons, new empirical fits, extraction of L-subshell ionization cross sections with various atomic parameters, and their comparison with the ECPSSR theory and its modifications: a recommendation for reliable choice of atomic parameters and ionization theory for PIXE analysis. Journal of Physics: Conference Series, 2009, 194, 082008.	0.4	0
105	Development of a coincidence system for the measurement of X-ray emission atomic parameters. , 2013, , .		0
106	Background considerations in the analysis of PIXE spectra by Artificial Neural Systems Journal of Physics: Conference Series, 2016, 720, 012053.	0.4	0
107	Inter-annual variability of ice nucleating particles in Mexico city. Atmospheric Environment, 2022, 273, 118964.	4.1	Ο